Chapter 14

RADIO OBSERVATIONS OF THE QUIET SUN

Christoph U. Keller
National Solar Observatory, 950 N. Cherry Ave., Tucson, AZ 85719, USA
ckeller@noao.edu

Säm Krucker
Space Sciences Laboratory, University of California, Berkeley, CA 94720, USA
krucker@ssl.berkeley.edu

Abstract While radio observations of the Sun have mostly focused on active region phenomena, they also contribute unique data to our knowledge of the quiet Sun, in particular through accurate measurements of the temperature as a function of height in the atmosphere and through the measurement of nonthermal emissions from chromospheric and coronal heating events. Here we review observations of the quiet Sun using radio telescopes and discuss current science problems that will be addressed with future facilities such as the Frequency Agile Solar Radiotelescope (FASR).

Keywords: quiet Sun, temperature structure, coronal heating, prominence, filament, coronal hole

1. Introduction

An article on the quiet Sun needs to start with a definition of the term "quiet Sun." This is particularly important for radio observations that cover a large range of radial distances from the solar surface. In the context of the present review, we define the quiet Sun as those phenomena in the solar atmosphere that are not related to active regions. It therefore includes stationary structures such as coronal holes and quiescent filaments and prominences as well as transient phenomena such as those believed to be associated with heating of the transition region and the corona above the quiet photosphere.

Studying the quiet Sun has advantages over trying to grasp the complex phenomena in active regions because one deals with less complex magnetic field topologies and a supposedly simpler structure of the stratified atmosphere. In the photosphere and parts of the chromosphere, the quiet Sun is dominated by phenomena related to convection. Any energy input to the nonthermal heating of the upper chromosphere and corona in the quiet Sun must ultimately have the convective energy as its origin. Magnetic fields are considered to be the most likely channels for transporting the energy from the photosphere through the chromosphere and the transition region into the corona.

While most solar radio observations have focused on active region phenomena such as flares and coronal mass ejections, there are several areas in which the radio regime provides particularly important diagnostic capabilities to address questions regarding the quiet Sun:

- Radio observations provide a linear thermometer that can be scanned in height by changing the frequency of the observations;
- Radio observations show nonthermal heating events in the quiet upper chromosphere, the transition region, and the corona;
- Radio observations of the circular polarization are sensitive to the line-of-sight component of the coronal magnetic field.

We will discuss these areas in detail in the following sections. Radio observations of the quiet Sun have also been used to study problems associated with oscillations (e.g. Tsvetkov 1986; Borovik *et al.* 1997), but we will not discuss these observations any further because they have so far not led to fundamentally new insights about the quiet Sun.

Recent reviews of quiet Sun radio physics can be found in the 1998 proceedings of the Japanese National Radio Observatory conference (Bastian *et al.* 1999). In particular, Shibasaki (1999) reviewed microwave (10–30 GHz) and Lantos (1999) reviewed low-frequency (30–400 MHz) quiet Sun studies. Here we concentrate on the higher frequencies and discuss the more recent literature that has appeared since those reviews were prepared.

We start with short discussions of general issues associated with radio observations of the quiet Sun and list present and future radio telescopes that are suitable for quiet Sun studies. The majority of this chapter is divided into three areas: observations of the thermal emission from the quiet Sun to determine average atmospheric properties, observations of quiescent prominences and filaments, and observations of nonthermal emission thought to be connected with heating of the chromosphere and the corona.

2. Observing the quiet Sun at radio wavelengths

Radio emission from the quiet Sun is in the form of continuum radiation without significant spectral lines (but see Dravskikh & Dravskikh 1988 and Boreiko & Clark 1986). The lack of significant spectral lines is no surprise because the emission of plasma waves by atoms is more effective than the emission of ordinary photons in a turbulent plasma (e.g. Kaplan *et al.* 1977). Furthermore, collisional broadening of the closely-spaced energy levels that would be involved at radio wavelengths inhibits bound-bound transitions.

The absence of spectral lines limits the diagnostic capabilities of radio observations. On the other hand, the absence of complicated atomic and radiative transfer processes makes calculations much more simple. Nevertheless, wideband spectra of the intensity and the circular polarization with high temporal resolution are a powerful tool to retrieve physical parameters of the underlying atmosphere. Combinations of radio observations with X-ray, EUV, and optical measurements provide a particularly powerful tool (see Chapter 13 by Brosius).

Radio observations at the shortest wavelengths (sub-millimeter) have historically been performed with single-dish antennas and have therefore been limited in spatial resolution to tens of arcsec, except for those that have been recorded during a solar eclipse, which provides sub-diffraction-limited resolution in one dimension. Interferometric submillimeter arrays that can be pointed at the Sun are under construction (e.g. the Atacama Large Millimeter Array, ALMA), and they will open a new world for solar radio physics because of the sub-arcsecond spatial resolution that they will achieve.

At longer wavelengths many general purpose imaging radio interferometers are useful for studying the quiet Sun with good spatial resolution and high dynamic range, which is required to separate the rather weak signal of the quiet Sun from the strong active region signals that often dominate the measured signals. Since the quiet Sun contains a large number of sources that vary on time scales of minutes, many baselines and therefore many antennas are needed. Earth-rotation synthesis is normally not an option because the solar sources are not constant for a long enough period. Apart from the number of baselines and the receiver noise, the achieved image quality also depends on the accuracy with which phases and amplitudes can be calibrated. Self-calibrating schemes can be very useful to reduce antenna-based phase and amplitude errors, making use of redundancy when a large number of baselines are measured.

The Japanese Nobeyama Radioheliograph is currently the most powerful, solar-dedicated imaging radio telescope. It provides full disk maps of the Sun simultaneously at frequencies of 17 and 34 GHz, with an angular resolution of 10 and 5 arcsec, respectively, and with a time resolution as short as 0.1 seconds. At 17 GHz, both left and right-hand circularly polarized emission is recorded. The array consists of three arms with 28 antennas each. While originally built

to study flare-associated phenomena, it is well suited for full-disk quiet Sun studies (Shibasaki 1999).

The French solar-dedicated Nançay Radioheliograph consists of a cross-shaped 43-antenna array that images the Sun at 6 frequencies between 164 MHz and 432 MHz at a rate of 5 Hz (Avignon *et al.* 1989). These frequencies originate in the corona at heights of 0.1 to 0.5 solar radii above the photosphere.

The general purpose Very Large Array (VLA) in the United States with its 27 antennae in a Y-shaped array is successfully used to observe the Sun when it is in its most compact configurations. There are seven fixed observing wavelengths at 90, 20, 6, 3.6, 2.0, 1.3, and 0.7 cm. Circular and linear polarization measurements can be performed. The VLA is currently being expanded to the Expanded VLA (EVLA). While the addition of far-away antennas does not provide any advantages to solar observations, the much improved spectroscopic capabilities, allowing observations anywhere between 1 and 50 GHz and with more than 250,000 channels, will provide a fantastic solar capability. Its drawbacks include a low duty-cycle on the Sun due to its non-solar-dedicated nature, its limited field of view, and its relatively slow (of order 30 s) change of frequency bands.

The Russian RATAN-600 telescope has a circular arrangement of 895 antenna-segments that operate between 0.61 and 30 GHz. The large frequency range makes it attractive for solar observations in general, but the one-dimensional scans provide only limited information about the structure of the quiet Sun.

The solar-dedicated Owens Valley Solar Array (OVSA) in the United States consists of two 27-m and five 2-m antennae spreading over an area about 1.2 km wide. The receivers can tune to any harmonic of 200 MHz in the range of 1 to 18 GHz, and acquire phase lock in less than 10 ms. The system records left- and right-circularly polarized and linearly polarized radiation. The rapidly tuning receiver system provides near-simultaneous observations of an area of the Sun at many frequencies, allowing observations that require spectroscopic capabilities.

The planned Frequency Agile Solar Radiotelescope (FASR) is a Fourier synthesis telescope designed to perform imaging spectroscopy over an extremely broad frequency range (0.1–30 GHz). The frequency, temporal, and angular resolution of the instrument will be optimized for the many and varied radio phenomena produced by the Sun. Consequently, FASR will the most powerful and versatile radioheliograph ever built. FASR will probe all phenomena in the solar atmosphere from the mid-chromosphere to the outer corona.

The international Atacama Large Millimeter Array (ALMA) is currently under construction in the Chilean Andes. Its 64 antennas can observe in all wavelength ranges between 0.35 and 10 mm that are transmitted by the Earth's atmosphere. Its spatial resolution of down to $0.01''$as well as its spectroscopic

capabilities should make it particularly interesting for solar observations (Bastian 2002).

3. General appearance of the quiet Sun in radio waves

Radio observations are particularly useful for temperature measurements as a function of optical depth because higher frequencies arise from lower layers of the solar atmosphere. Radio waves of a certain frequency can only be observed from regions where the local electron plasma frequency ν_p is equal to or lower than the radio frequency ν. Since the electron density decreases with height, ν_p also decreases with height. Radio observations therefore provide diagnostic data from the chromosphere out to the heliosphere. The lower chromosphere is seen at frequencies of 100–1000 GHz, the middle chromosphere is seen at 20–100 GHz, and the upper chromosphere is seen at frequencies of 2–20 GHz. The corona is seen at frequencies of 2 GHz and below.

At frequencies above 10 GHz, the Sun appears as a rather uniform disk with a brightness temperature of about 11,000 K (see Figure 14.1). Active regions show up as somewhat brighter areas. At frequencies of about 1 GHz, the quiet Sun has a brightness temperature of about 50,000 K, while active regions show brightness temperatures of a few million K, which is due to the coronal component. In coronal holes, the coronal contribution is very small while it may be substantial elsewhere in the quiet Sun. Coronal holes therefore show up as darker areas below about 10 GHz. Paradoxically, coronal holes appear brighter than the quiet Sun (Nindos *et al.* 1999a) at frequencies above about 10 GHz, for reasons that are not well understood. At 0.1 GHz and below, the whole Sun has a brightness temperature of about one million K, and active regions are no longer distinguishable, but higher-laying structures such as coronal streamers show up as bright structures.

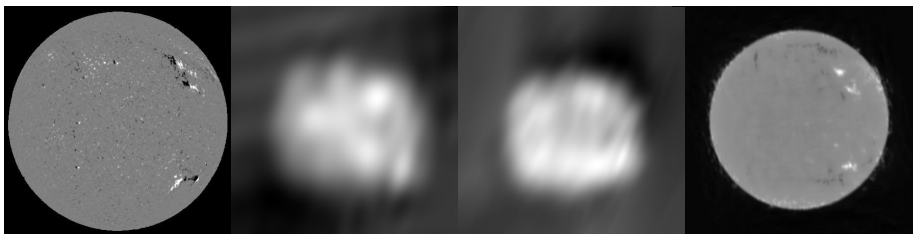

Figure 14.1. The quiet Sun on 1998 February 01 at different radio wavelengths, compared with a photospheric magnetogram. From left to right: Kitt Peak magnetogram, Nançay Radioheliograph at 164 and 327 MHz, and Nobeyama Radioheliograph at 17 GHz.

3.1 Submillimeter observations

Radio images of the Sun at the shortest wavelengths have been obtained at 0.85 mm (a wavelength where the Earth's atmosphere transmits well at high altitudes) with the James Clerk Maxwell Telescope (JCMT) on Mauna Kea (Lindsey *et al.* 1990) and the 10.4 m Caltech Submillimeter Observatory (Bastian *et al.* 1993). These submillimeter full-disk images of the Sun correlate well with images obtained in very strong spectral lines in the visible spectrum such as CaII K, which are again well correlated with maps of the magnetic field. At 0.85 mm, one therefore clearly sees the supergranular network (Lindsey & Jefferies 1991). The resolution of these observations is on the order of $20''$. A better spatial resolution can be obtained at the limb during a solar eclipse when the lunar limb acts as a moving knife-edge. This allows measurements of the limb profile with a spatial resolution of a few arcsec (Ewell *et al.* 1993), which shows a roughly 10% limb brightening in the outer $7''$and a radio limb that extends well beyond the visible limb.

3.2 Millimeter and microwave observations

The time-averaged brightness temperature images of the quiet Sun at frequencies of 5 to 20 GHz also show the chromospheric network (Bastian *et al.* 1996), such as shown in Figure 14.2. However, there are considerable temporal variations in the observed brightness temperature.

Coronal holes at the poles as well as elsewhere on the solar disk show enhanced emission between 17 and 87 GHz (see Nindos *et al.* 1999*b*, and references therein). Outside of this frequency range, the coronal holes either cannot be detected or show reduced emission because of the lower coronal temperature. The enhancement is due to both compact as well as diffuse sources within coronal holes.

At 17 GHz, the diffuse component has 1500 K excess brightness, and the compact sources show a localized excess brightness of about 3500 K (Nindos *et al.* 1999*b*). The cause of the enhancement is not well understood. A comparison of 17-GHz Nobeyama radio observations with simultaneous SOHO EIT images does not show a correlation between the compact radio sources and the bright EUV features (Nindos *et al.* 1999*b*). The temporal variations of the compact microwave sources also did not correspond to any significant changes in EUV emission. This suggests that the origin of the polar brightening is not coronal; it seems that the bulk of the patchy radio emission comes from heights below the 80,000 K layer.

Recent measurements of an equatorial coronal hole combining 17-GHz maps from the Nobeyama Radioheliograph with extreme-ultraviolet, far-ultraviolet, and visible emissions (Moran *et al.* 2001) also do not show an enhanced temperature as measured with UV lines. However, there are indications for an

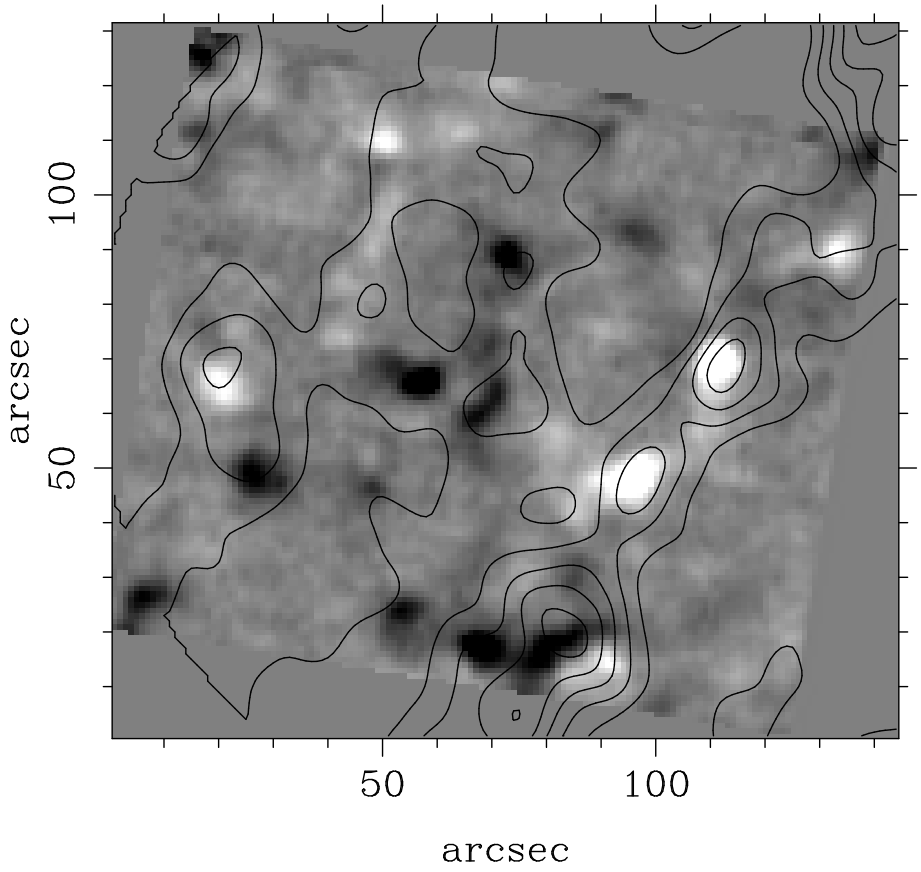

Figure 14.2. A magnetogram of the quiet Sun close to disk center obtained with ZIMPOL at the McMath-Pierce solar telescope with contour lines showing the 2-cm radio emission intensity as observed with the VLA.

increased Hα intensity in radio enhancements. No such enhancements in Hα were detected in the coronal hole outside of radio enhancement regions. This indicates that areas of increased Hα intensity are responsible for the enhanced radio emission and place the origin of the radio enhancement in the chromosphere. At 37 and 87 GHz, the enhanced radio emission in the polar areas is associated with polar faculae, indicating that they are different manifestations of the same underlying activity (Riehokainen *et al.* 2001).

Another interesting development of microwave observations of the quiet Sun has recently been opened by the development of the theory and observational tools to use the birefringence of the free-free emission to make radio magne-

tograms at the base of the quiet Sun corona (Grebinskij *et al.* 2000, see also Chapter 6 by Gelfreikh).

4. Thermal stratification of the quiet Sun

Measuring the temperature stratification of the solar atmosphere has traditionally been done using spectral lines in the optical regime. However, the temperature dependence of spectral line shapes is often highly nonlinear, which requires extensive atomic and radiative transfer modeling to deduce temperatures. The problem becomes particularly severe for very strong lines such as the Ca II H and K lines that are formed in the lower chromosphere. The formation of these lines cannot be assumed to occur in local thermal equilibrium (LTE). The line core that is formed highest in the atmosphere is dominated by the local radiation field and becomes independent of the local temperature. Temperature measurements using strong lines in the visible spectrum as well as EUV lines are therefore not good temperature diagnostics of the upper photosphere and the lower chromosphere. The infrared continuum provides a good measurement of the temperature throughout the photosphere because of the simple relation between the local temperature at optical depth unity and the infrared continuum formation, which is dominated by the H^- opacity and is rather devoid of spectral lines.

In the quiet Sun, thermal free-free (also called thermal bremsstrahlung), which is due to individual electrons being accelerated by the Coulomb field of ions, is the main emission mechanism at radio wavelengths. This incoherent radiation comes mainly from an optically thick source. Therefore the measured intensity only depends on the temperature of the emitting electrons.

In solar radio physics, observed (unpolarized) intensities are expressed in terms of the brightness temperature T_b, which is defined as

$$T_b = \frac{I_\nu c^2}{2k_B\nu^2} \ , \tag{14.1}$$

with c being the speed of light, k_B the Boltzmann constant, and I_ν the intensity observed at the frequency ν. For a given atmospheric stratification, the brightness temperature of the quiet sun is thus given by

$$T_b = \int_0^{\tau_{max}} T e^{-\tau} d\tau \ , \tag{14.2}$$

where T is the temperature, τ is the optical depth, and τ_{max} is a suitably large optical depth, typically $\gg 1$. The optical depth is the integral of the absorption coefficient, κ, along the line of sight. An extensive treatment of the subject can been found in Dulk (1985). Assuming a frequency of 0.1 GHz and a temperature of 10^6 K, typical conditions for observing the solar corona, the

absorption coefficient κ is given by Dulk (1985) as

$$\kappa(\nu) = 0.2 n_e^2 T^{-\frac{3}{2}} \nu^{-2} (\mathrm{cm}^{-1}) \ . \tag{14.3}$$

To calculate the bremsstrahlung emission from a model atmosphere with a known temperature and the electron density stratification, one calculates the absorption coefficient and integrates it from the top of the model along the line of sight to obtain the optical depth τ as a function of geometrical height. The temperature can then be expressed as a function of optical depth, and the integration along the line of sight can be carried out. For oblique paths such as when calculating the center-to-limb variation, the cosine of the heliocentric angle has to be taken into account in the calculation of the optical depth and the integration over the temperature stratification. Very close to the limb, the curvature of the atmosphere also has to be taken into account.

This approach has historically been taken to test models of the quiet Sun. The observed and the predicted brightness temperatures as a function of frequency and center to limb distance are compared. The models can then be tuned to minimize the difference between observations and theoretical prediction. Unfortunately, the temperature stratification cannot be directly deduced from radio measurements because the latter do not provide a measure of the optical depth or opacity. Either one makes certain assumptions or uses additional observations to estimate the opacity.

Another limitation of the one-dimensional line-of-sight approach outlined above becomes evident when dealing with optically thick, filamentary objects such as prominences at the limb that are also seen as filaments on the disk. Because of the filamentary nature of the prominences, only a fraction of the emission in the spatial resolution element comes from the optically thick prominence. This fraction is called the filling factor, and it influences the interpretation of the observed brightness temperature. Unfortunately, radio observations alone are insufficient to determine the filling factor without making additional assumptions. Yet another limitation has to do with optically thin structures such as hot plasma in quiet Sun coronal loops. The increase in brightness temperature due to the optically thin, hot plasma only goes as one over the square root of the plasma temperature, which is rather insensitive. The quiet Sun radio emission therefore has two contributions: one from the optically thin corona, and one from the layer where optical depth unity is reached.

Models of the average quiet Sun have often made use of the measured center-to-limb variation of the absolute brightness temperature (e.g. Vernazza *et al.* 1976). These models are one-dimensional, hydrostatic models that balance the heat flux and the radiative losses. As far as microwave brightness temperatures are concerned, the FAL model C (Fontenla *et al.* 1993) fits the data best. Measurements between 1.4 and 18 GHz (Zirin *et al.* 1991) indicate that the

measured brightness temperature of the quiet Sun between 1.4 and 10 GHz can be modeled by an optically thick component in the chromosphere and an optically thin coronal component. Above 10 GHz, the transition region needs to be taken into account, and spatial variations become important. Furthermore, the phase of the solar cycle must be considered since the coronal contribution increases during periods of high solar activity even in the quiet Sun (Bastian *et al.* 1996).

However, all of these static models ignore the fact that the upper solar atmosphere is highly dynamic and spatially structured. Microwave observations tend to show the cooler structures in the chromosphere because the measured brightness temperature (Bastian *et al.* 1996) is well explained by a chromospheric model that can reproduce the carbon monoxide lines originating from the cool part of the chromosphere (e.g. Avrett 1995). Indeed, until very recently, temperature stratifications of the quiet Sun derived from UV spectral line intensities by far overestimate the observed radio brightness temperature (Zirin *et al.* 1991). By differently analyzing the UV line intensities and distinguishing network and cell-interior as different contributions to the measured radio brightness temperature, it has finally been possible to bring the UV and the radio measurements into agreement (Landi & Chiuderi Drago 2003).

5. Filaments and prominences

Filaments and prominences are different manifestations of the same phenomenon. Filaments are prominences seen on the solar disk. They can be well observed in the microwave domain because they are optically thick at those frequencies. This makes radio observations very suitable for estimating the temperature in filaments. Indeed, radio observations are much better than the traditional Hα observations because the former do not suffer from Doppler shifts and rather complicated spectral line formation processes. Filaments typically occur over extended neutral lines in the quiet Sun and show temperatures well below the temperature of the surrounding quiet corona. Filaments can be quiescent or they can erupt. Since the Hα line is rather limited in temperature range, only radio observations can follow an erupting filament from its quiescent state at temperatures of about 10^4 K to the ambient coronal temperature of the order of 10^6 K.

The first simultaneous radio and EUV observations of a filament (Chiuderi Drago *et al.* 2001) showed that the Lyman continuum absorption is responsible for the lower intensity observed above the filament in the EUV lines that are formed in the transition region. The lower intensity of coronal lines and the depression in brightness temperature at radio wavelengths is due to the lack of

coronal emission. These observations are consistent with a prominence model of cool threads embedded in the hot coronal plasma, with a sheath-like transition region around them.

Hanaoka *et al.* (1999) used the Nobeyama array at 17 GHz to measure the temperature of erupting filaments on the disk. They found that the brightness temperature of the filaments increases to the temperature of the quiet Sun at the beginning of the abrupt eruptions, while the filaments keep their large optical thickness. After the rapid increase, the brightness temperature does not change significantly while the filaments erupt. Heating of the surface of the cool core of the prominences up to the transition-region temperature is the most plausible explanation of the observed increase in the brightness temperature at 17 GHz.

Marqué & Lantos (2002) used the Nançay Radioheliograph to detect brightness depressions around filaments, which are believed to be the signature of a coronal cavity that surrounds the filament. After a filament erupts, even when signatures of only minor energy release are present, the decimetric observations indicate the coronal restructuring on the disk that follows the filament eruption. This suggests the close relation of filament eruptions and coronal mass ejections (see also Chapter 11 by Vourlidas).

6. Coronal heating events in the quiet Sun

More than fifty years after the million-Kelvin temperatures in the corona had been discovered, their cause is still not settled. Many heating mechanisms have been proposed (see the reviews in Ulmschneider *et al.* 1991), including a very large number of discrete heating events in the form of very small flares (microflares and/or nanoflares), various types of waves, and continuous electric currents. While radio observations have been used for almost two decades to study coronal heating events in the quiet Sun, the combination of sensitive radio observations with powerful EUV and X-ray instruments in space has provided us with new insight. Here I will concentrate on summarizing some of the important developments during the last five years.

Initial indications for a relation between compact radio sources in the quiet Sun and coronal brightenings were based on an apparent association of enhanced radio emission with HeI 1083 nm dark points (a proxy for X-ray bright points) at 20 cm (Habbal *et al.* 1986, Habbal & Harvey 1988) and at 6 cm (Fu *et al.* 1987). Sources seen in HeI 1083 nm and at radio wavelengths have been observed to change on time scales of a few minutes. Nevertheless, there were always many more HeI 1083 nm dark points observed than radio sources.

A direct relation between X-ray and radio measurements was first reported by Nitta *et al.* (1992) at 20 cm and by Kundu *et al.* (1994) at 2 cm. About half of the sources seen as enhanced features at radio wavelengths correspond to

X-ray bright points. The other half seems to be associated with concentrated unipolar magnetic flux (e.g. Nitta *et al.* 1992). The temperature of these areas as deduced from X-ray measurements is on the order of 1–2$\times 10^6$ K, while the radio brightness temperature is about a factor of 20 less because the sources are optically thin at radio wavelengths. X-ray bright points tend to be associated with two magnetic elements of opposite polarity that evolve together (e.g. Harvey 1985).

A weak correlation between enhanced radio emission and the magnetic network was discovered by Kundu *et al.* (1988) and Gary & Zirin (1988) at 20 cm. The correlation becomes much better at 6 cm and shorter wavelengths. As seen before, radio emission at these wavelengths originates predominantly from the upper chromosphere with the corona making only a small contribution. Discrete radio sources in the chromospheric network are variable on time scales of a few minutes (Gary & Zirin 1988; Gary *et al.* 1990), such as in Figure 14.3. Nevertheless, the overall evolution of the radio emission is consistent with the evolution of the supergranular network itself (Bastian *et al.* 1996).

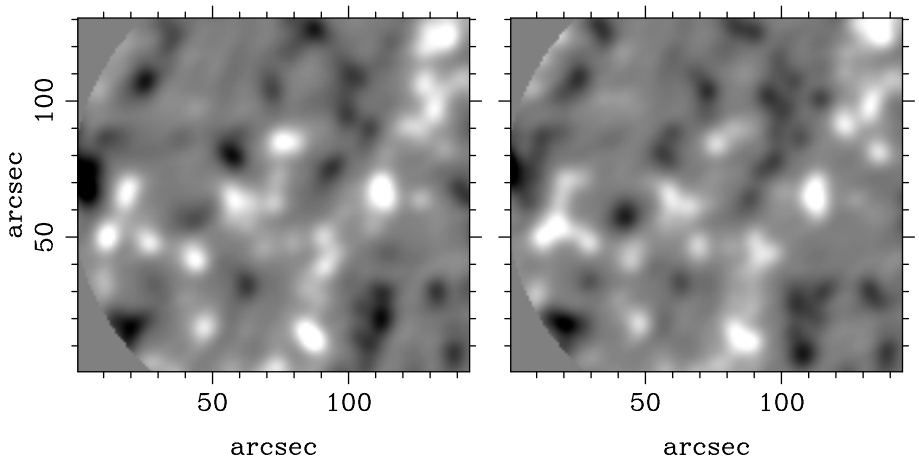

Figure 14.3. Two radio maps of the quiet Sun obtained with the VLA at 2 cm spaced 2 minutes apart.

Benz *et al.* (1997) compared long-exposure soft X-ray images from Yohkoh with VLA maps at 3.6, 2, and 1.3 cm and photospheric magnetograms. Their X-ray observations are more than three orders of magnitude more sensitive than previous observations of X-ray bright points. They find that soft X-ray sources are often associated with bipolar features in the magnetogram, similar to the much brighter X-ray bright points. As previous authors had reported, they find the best correlation between the magnetogram and the radio observations at the shortest wavelengths which originate from the deepest atmospheric layers. The

correlation decreases for the longer wavelengths coming from higher layers, and is also not pronounced for the soft X-ray photons, which originate exclusively from the corona. Interestingly, the X-ray and radio emissions observed close to disk center are often displaced by a few arcsec, indicating inclined magnetic field lines.

Krucker *et al.* (1997) studied the temporal variations in the soft X-ray and radio emissions (see Figure 14.4) using the same data set as Benz *et al.* (1997). X-ray brightenings of at least an order of magnitude less than previous observations show a corresponding radio source correlating in space and time. The authors call these events *network flares* because of the similarities they share with standard solar flares: Variations in temperature and emission measure during the soft X-ray enhancements are consistent with evaporation of cooler material from the transition region and the chromosphere; the ratio of the total energies radiated in X-rays and at radio frequencies is similar to that observed in flares, at least one of the four radio events shows a degree of polarization as high as 35%; in three out of four cases the centimeter radio emission peaks several tens of seconds earlier than in the X-ray emission; and the associated radio emission tends to be more structured and to have faster rise times.

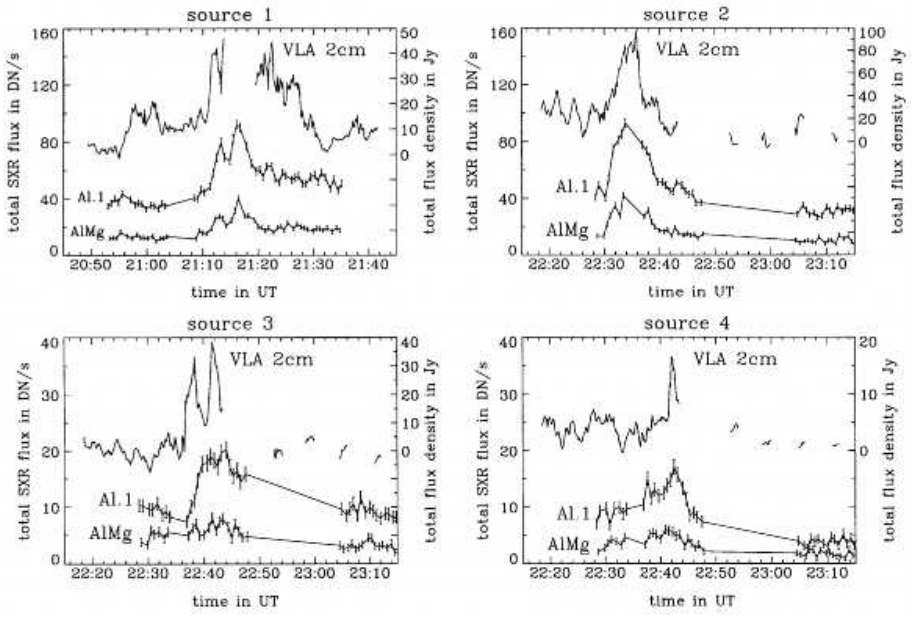

Figure 14.4. Comparison of network flares in soft X-ray and radio waves at 2 cm (from Krucker *et al.* (1997).

In contrast, Nindos *et al.* (1999) selected transient radio brightenings at frequencies between 0.33 and 4.5 GHz and compared them with soft X-ray images from Yohkoh and SOHO EIT images. While most of the events were related to active regions, one of the cases was clearly in the quiet Sun. All events were consistent with the radio emission being due to nonthermal, mildly relativistic electrons.

Benz & Krucker (1999) extended their previous work on the temporal evolution of microflares by statistically studying the faintest fluctuations in the corona and relating them to the layers below. They combined VLA observations with SUMER, CDS, EIT, and MDI data from SOHO. Their analysis indicates that the first emissions due to coronal events occur in spectral lines originating in the transition region and the upper chromosphere. These emissions are assumed to be due to electron beams impinging on the chromosphere. The coronal line EUV emission lags by about 5 minutes, similar to what is seen in regular flares. This coronal line emission is likely due to the evaporating plasma expanding into the corona. The temporal correlation of the radio measurements with respect to the other observations is not as well established. The authors suggest the presence of two different emission processes at work radiating both thermal emission and nonthermal gyrosynchrotron emission at various fluxes. Their statistical results show that the coronal heating events follow the properties of regular solar flares and thus may be interpreted as microflares or nanoflares.

Similar comparisons between radio and transition region lines also indicate the similarity of network flares and the much larger active-region flares (Krucker & Benz 2000). The differences between these two types of flares seem to be mainly quantitative, and the relatively large heating events may in principle be considered as microflares or large nanoflares, thus small versions of regular flares.

7. FASR and the quiet Sun

FASR will provide many new capabilities to answer important questions about the Sun. From a technical point of view, the fact that FASR will be a solar-dedicated instrument should not be underestimated. Past and current combined observing runs between space-based assets and ground-based optical and radio-telescopes are very difficult to arrange because the allocation of observing time on non-solar-dedicated radio telescopes is inflexible. If one wants to study a certain quiet Sun phenomenon such as a filament, one has at most a few days between noticing the interesting object and the time that observations have to be carried out. Furthermore, one often only gets a few hours observing time at telescopes such as the VLA, which might not be sufficient for the event to happen that one would like to study (e.g. the eruption of a filament).

In addition to the flexible scheduling of FASR, its full-disk capability is another advantage for quiet Sun studies. In particular when active regions are also present on the solar disk, a restricted field of view will always suffer to some degree from signals outside of the field of view, which can be very strong in the case of active regions.

From a scientific point of view, the large simultaneous wavelength coverage and the spectral capabilities of FASR will allow new approaches to quiet Sun studies. For instance, using the birefringence of the free-free emission at various frequencies, one will be able to obtain magnetograms at the corresponding levels in the upper solar atmosphere, something that is not feasible with any other known approach.

FASR will also have an impact on modeling of the quiet solar atmosphere. By the time that FASR will be operational, the quiet Sun must be modeled as a time-dependent, three-dimensional atmosphere that is permeated by magnetic fields. The one-dimensional hydrostatic models that are still used today will not be sufficient to explain FASR observations of the quiet Sun. It is therefore important that, along with the development and construction of FASR, the necessary modeling tools are developed to interpret the data to be delivered by FASR.

Current riddles posed by the quiet Sun that will be addressed by a combination of FASR and other ground and space-based assets include:

- What is the magnetic field topology above the photosphere?
- How is energy moved from the photosphere through the chromosphere and transition region into the corona?
- What determines the location of filaments and filaments channels, what is their structure, and what determines their stability?
- What are spicules?
- How is magnetic flux removed (an important ingredient in any solar dynamo theory)?

Acknowledgments

CUK acknowledges support from the Humboldt Foundation while finishing this chapter. The National Solar Observatory is operated by the Association of Universities for Research in Astronomy (AURA), Inc. under cooperative agreement with the National Science Foundation.

References

Avignon, Y., Bonmartin, J., Bouteille, A., Clavelier, B. & Hulot, E. 1989, Solar Phys, 120, 193

Avrett, E. H. 1995, In Infrared tools for solar astrophysics: What's next?, p303
Bastian, T. S. 2002, Astronomische Nachrichten, 323, 271
Bastian, T. S., Dulk, G. A. & Leblanc, Y. 1996, ApJ, 473, 539
Bastian, T. S., Ewell, M. W. & Zirin, H. 1993, ApJ, 415, 364
Bastian, T. S., Gopalswamy, N. & Shibasaki, K., editors 1999, Solar Physics with Radio Observations
Benz, A. O., Krucker, S., Acton, L. W. & Bastian, T. 1997, A&A, 320, 993
Benz, A. O. an Krucker, S. 1999, A&A, 341, 286
Boreiko, R. T. & Clark, T. A. 1986, A&A, 157, 353
Borovik, V. N., Livshitz, M. A. & Medar', V. G. 1997, Astronomy Reports, 41, 836
Chiuderi Drago, F., Alissandrakis, C. E., Bastian, T., Bocchialini, K. & Harrison, R. A. 2001, Solar Phys, 199, 115
Dravskikh, A. F. & Dravskikh, Z. V. 1988, Soviet Astronomy, 32, 104
Ewell, M. W., Zirin, H., Jensen, J. B. & Bastian, T. S. 1993, ApJ, 403, 426
Fontenla, J. M., Avrett, E. H. & Loeser, R. 1993, ApJ, 406, 319
Fu, Q., Kundu, M. R. & Schmahl, E. J. 1987, Solar Phys, 108, 99
Gary, D. E. & Zirin, H. 1988, ApJ, 329, 991
Gary, D. E., Zirin, H. & Wang, H. 1990, ApJ, 355, 321
Grebinskij, A., Bogod, V., Gelfreikh, G., Urpo, S., Pohjolainen, S. & Shibasaki, K. 2000, A&AS, 144, 169
Habbal, S. R. & Harvey, K. L. 1988, ApJ, 326, 988
Habbal, S. R., Ronan, R. S., Withbroe, G. L., Shevgaonkar, R. K. & Kundu, M. R. 1986, ApJ, 306, 740
Hanaoka, Y. & Shinkawa, T. 1999, ApJ, 510, 466
Harvey, K. L. 1985, Australian Journal of Physics, 38, 875
Kaplan, S. A., Kleiman, E. B. & Oiringel, I. M. 1977, Soviet Astronomy, 21, 742
Krucker, S. & Benz, A. O. 2000, Solar Phys, 191, 341
Krucker, S., Benz, A. O., Bastian, T. S. & Acton, L. W. 1997, ApJ, 488, 499
Kundu, M. R., Schmahl, E. J. & Fu, Q.-J. 1988, ApJ, 325, 905
Kundu, M. R., Shibasaki, K., Enome, S. & Nitta, N. 1994, ApJ, 431, L155
Landi, E. & Chiuderi Drago, F. 2003, ApJ, 589, 1054
Lantos, P. 1999, In Proceedings of the Nobeyama Symposium, held in Kiyosato, Japan, Oct. 27-30, 1998, Eds.: T. S. Bastian, N. Gopalswamy & K. Shibasaki, NRO Report No. 479., p.11-24, pages 11
Lindsey, C. A. & Jefferies, J. T. 1991, ApJ, 383, 443
Lindsey, C. A., Yee, S., Roellig, T. L., Hills, R., Brock, D., Duncan, W., Watt, G., Webster, A. & Jefferies, J. T. 1990, ApJ, 353, L53
Marque, C. & Lantos, P. 2002, In SF2A-2002, Semaine de l'Astrophysique Francaise

Moran, T., Gopalswamy, N., Dammasch, I. E. & Wilhelm, K. 2001, A&A, 378, 1037

Nindos, A., Kundu, M. R. & White, S. M. 1999a, ApJ, 513, 983

Nindos, A., Kundu, M. R., White, S. M., Gary, D. E., Shibasaki, K. & Dere, K. P. 1999b, ApJ, 527, 415

Nitta, N., Bastian, T. S., Aschwanden, M. J., Harvey, K. L. & Strong, K. T. 1992, PASJ, 44, L167

Riehokainen, A., Urpo, S., Valtaoja, E., Makarov, V. I., Makarova, L. V. & Tlatov, A. G. 2001, A&A, 366, 676

Shibasaki, K. 1999, In Proceedings of the Nobeyama Symposium, held in Kiyosato, Japan, Oct. 27-30, 1998, Eds.: T. S. Bastian, N. Gopalswamy & K. Shibasaki, NRO Report No. 479., p.1-9, p1

Tsvetkov, L. I. 1986, Izvestiya Ordena Trudovogo Krasnogo Znameni Krymskoj Astrofizicheskoj Observatorii, 75, 77

Ulmschneider, P., Priest, E. R. & Rosner, R., editors 1991, Mechanisms of Chromospheric and Coronal Heating

Vernazza, J. E., Avrett, E. H. & Loeser, R. 1976, ApJ Supp., 30, 1

Zirin, H., Baumert, B. M. & Hurford, G. J. 1991, ApJ, 370, 779